Preprints of the 18th IFAC World Congress
Milano (Italy) August 28 - September 2, 2011

Nanopositioning for Storage Applications

Evangelos Eleftheriou

IBM Research - Zurich, 8803 Rüschlikon, Switzerland
(e-mail: ele@zurich.ibm.com)

Abstract: In nanotechnology applications, nanopositioning, i.e., nanometer-scale precision control at dimensions of less than 100 nm, plays a central role. One can view nanopositioners as precision mechatronics systems aiming at moving objects over a certain distance with a resolution that could be as low as a fraction of an Ångström. Actuation, position sensing and feedback control are the key components of nanopositioners that determine how successfully the stringent requirements on resolution, accuracy, stability, and bandwidth are achieved. Historically, nanopositioning has played a critical role in scanning probe microscopy (SPM), and it appears that it will play a crucial role in emerging applications such as lithography tools and semiconductor inspection systems, as well as in molecular biology, nanofabrication, and nanomanufacturing. Moreover, it is becoming an important requirement in storage systems, ranging from novel probe-based storage devices to mechatronic tape-drive systems, to support the high areal density or storage capacity needs. This paper will review control-related research in nanopositioning for two extreme cases of data-storage systems, namely, in probe and in tape storage.

1. INTRODUCTION

THE PAST two and a half decades have witnessed the emergence and explosive growth of nanoscience and nanotechnology (Crandall, 1996; Bushan, 2004; Shapiro, 2005; Sheetz *et al.*, 2005). In all these applications, nanopositioning, i.e., nanometer-scale precision control at dimensions of less than 100 nm, plays a central role. One can view nanopositioners as precision mechatronics systems aiming at moving objects over a certain distance with a resolution that could be as low as a fraction of an Ångström.

Manipulation and interrogation at the nanometer scale with a scanning probe microscope (SPM) necessitate positioning systems with atomic-scale resolution (Wiesendanger, 1994; Yves, 1995). Nanopositioning is, for example, needed to scan the probe over a sample during surface imaging and to control the interaction between probe and sample surface during surface interrogation and modification. Nanopositioning systems are also at the core of future lithography tools that might replace the ubiquitous optical lithography systems (Vettiger *et al*., 1996), and novel nanopositioning tools are also needed for the positioning of wafers, mask alignment, and semiconductor inspection systems (Harriot, 2001; White and Wood, 2000; Verma *et al*., 2005).

Furthermore, they are vital in molecular biology for imaging, alignment, and nanomanipulation as required, for example, in cell tracking and DNA analysis, nanomaterials testing (Bushan, 1995; Kalinin and Bonnell, 2000), nanoassembly (Whitesides and Love, 2001), and the manufacturing of small objects (Meldrum *et al.*, 2001). Such nanopositioning systems are also crucial in optical alignment systems (Rihong *et al.*, 1998; Krogmann *et al.*, 1999). Finally, nanometer-scale precision is required for probe-storage devices with areal densities higher than 1 Tb/in^2 (Hosaka *et al.*, 1997; Sebastian *et al.*, 2008a), for the servo system of hard-disk drives (HDD) (Jianxu and Ang, 2000; Horowitz *et al*., 2004), and will soon also be needed for the servo system of tape drives (Berman *et al*., 2007; Argumedo *et al.*, 2008; Cherubini *et al.*, 2011).

This vast range of applications with such diverse operation conditions poses new challenges for the control of nanopositioning devices because they necessitate high resolution, high bandwidth, and robust control designs, see for example, Fleming and Moheimani (2003); Croft and Devasia (1999); Croft *et al.* (2001); Schitter *et al.* (2001); Salapaka *et al*. (2002); Sebastian and Salapaka (2005); El Rifai and Youcef-Tomie (2001), and Stemmer *et al.* (2005).

An extended survey of control issues in nanopositioning was presented in (Devasia *et al.*, 2007). In this paper, we will review control-related research in nanopositioning for two extreme cases of data storage systems, namely, in probe and in tape storage. Section 2 gives an overview of probe-storage applications, focusing on MEMS-based miniaturized as well as non-miniaturized actuator designs. Moreover, it discusses two position sensor technologies: thermal position sensors and new magnetoresistance-based position sensors. The last part of that section presents various control strategies. Section 3 discusses the other extreme — tape storage — and its importance for high-capacity archival applications. Current voice-coil head actuators as well as a novel high-bandwidth piezoelectric actuator design are presented. In addition, it discusses control schemes for reducing the position error signal (PES) of commercial tape drive systems to values close to 100 nm, tape system architectures, and perpendicularly-oriented media that could bring PES below 20 nm, thereby enabling high track densities and cartridge capacities. Finally, in Section 4, we draw conclusions.

2. PROBE TECHNOLOGIES

Nanopositioning is a key enabling technology for high-throughput scanning probe techniques. Subnanometer precision at fast rates is required in a wide range of

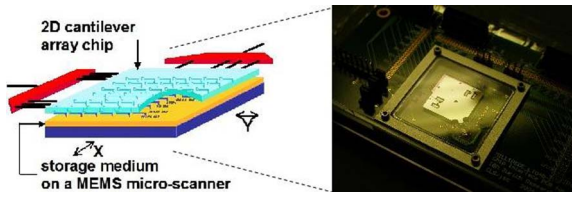

Fig. 1. Probe-based data-storage device prototype. From Sebastian *et al.* (2008a)

applications including probe-based data storage. Probe-based data storage is an alternative to magnetic storage and has been proposed for both mobile and archival applications because of its ultra-high areal density. Among the various concepts advanced, thermomechanical recording and retrieval of data encoded as nanometer-scale indentations in thin polymer films is arguably the most advanced (Vettiger *et al*., 2002; Eleftheriou *et al.*, 2003). A schematic illustrating the concept of a probe-based storage device as well as a photograph of a miniaturized device prototype are shown in Fig. 1. An array of thermomechanical probes is used to read and write information. The data are recorded as indentations on a thin polymer film, which acts as the storage medium. This concept, which originally targeted small form-factor and high-capacity memory applications, holds high promise for archival storage, in particular for applications requiring WORM functionality (Wright et al., 2006; 2008). In addition to polymer media and thermomechanical recording, also phase-change materials and conductive probes have been considered for this application (Bhaskaran et al., 2009). For archival applications, the form factor does not play a role and therefore there is no strong requirement for miniaturized actuators. However, in both data-storage applications, high bandwidth and high resolution nanopositioning are essential. This dual objective requires the design and development of novel sensors and actuators as well as suitable control strategies.

2.1. Actuators and position sensing

MEMS-based electromagnetic actuator and thermal position sensors. A miniaturized electromagnetic-actuator-based nanopositioner for small-form-factor probe-storage applications is shown in Fig. 2. It was used to provide *x*/*y*-displacement capabilities in the range of about 120 µm. This range is approximately 20% larger than the pitch between adjacent cantilevers in the array. Actuation is achieved by means of two voice-coil-type actuators, which provides a large travel range at low operating voltages compared with electrostatic

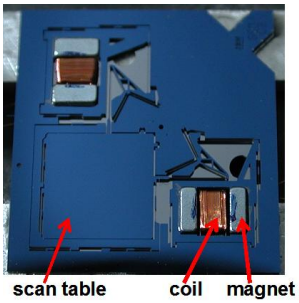

Fig. 2. Photograph of the microscanner. From Sebastian *et al.* (2008a)

or piezoelectric actuation. Each actuator consists of a pair of magnets mounted in the actuator frames. Upon application of a current to the coil, one magnet is attracted to the coil and the other is repelled by it, resulting in forces on the shuttle in the same direction. The net force induces a displacement of the shuttle that is related to the stiffness of the positioner. This motion is coupled to the scan table by means of a mass-balancing scheme, which makes the scanner robust against external shocks and vibrations. The nanopositioner achieves linear displacement as a function of the driving current and exhibits a low crosstalk of 1%–3% between the axes. This design is suitable for parallel-probe-based mobile storage devices and also as generic nanopositioning system for other nanotechnology applications (Lantz *et al.*, 2007).

Information on the *x*/*y* position of the microscanner is provided by two pairs of thermal position sensors in the form of relatively large microheaters, which are fabricated on the cantilever-array chip and positioned directly above the scan table such that they partially overlap the scan table, see Fig. 3. To sense a displacement of the object, the temperature dependence of the Si resistance is exploited. A fraction of the heat generated by the resistive heater is conducted through the ambient air into the scan table, which acts as a heat sink. A displacement of the scan table gives rise to a change in the efficiency of this cooling mechanism, resulting in a change in the heater temperature and thus in its electrical resistance. The sensors are driven by a constant voltage, and changes in the resulting current are measured with a current-to-voltage amplifier. To minimize drift effects, the sensors are operated in pairs using a differential configuration. Although these devices are quite simple, the linearity, noise limit, and drift performance that can be achieved are surprisingly good. Specifically, these sensors have a band–width of approx. 4 kHz and a displacement resolution of less than 1 nm over that bandwidth. The thermal sensors operate over the entire travel range of the microscanner and hence are capable of providing global position information (Lantz *et al*., 2005).

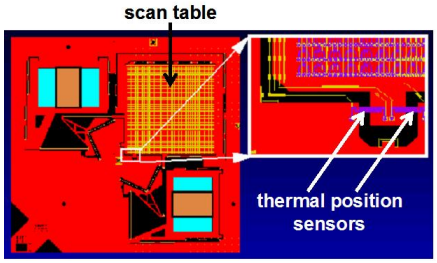

Fig. 3. Microscanner and thermal position sensors. From Sebastian *et al.* (2008a)

High-bandwidth piezoelectric actuator and magneto-resistance-based position sensors. For high-bandwidth nanopositioning, a suitable high-speed scanner should have high first resonances and a low coupling between the three orthogonal directions. A high-speed *x*/*y*-positioning scanner design was developed and is shown in a schematic form in Fig. 4. The combination of high stiffness/rigidity of the flexures and low carrier mass enables high first resonances to

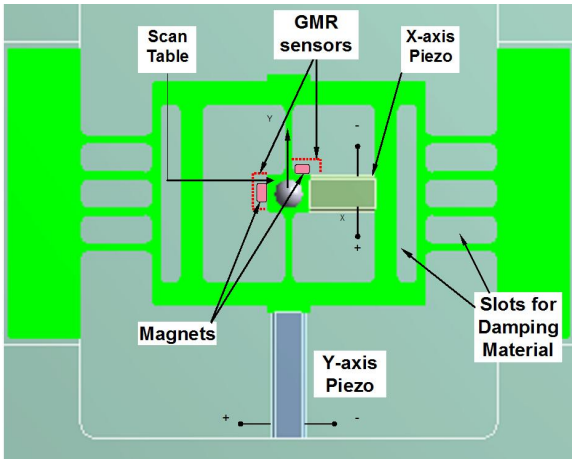

Fig. 4. Schematic depiction of *x*/*y* nanopositioning stage. From Kartik *et al.* (2010a)

be achieved. The low mass combined with direct, uncomplicated mechanical connections ensures good dynamical behavior and low directional cross-coupling. The scanner is fabricated from aluminum, and comprises one stage, actuated by piezoelectric stacks, in each the *x*- and the *y*-scan direction. Each piezo-stack was preloaded against the corresponding flexure. Provision was also made for passive damping of the flexure stages. The magnitude response of the scanner is remarkably flat up to the first resonance, which is at 4.1 kHz along the *x*-scan direction and at 4.77 kHz along the *y*-scan direction. The out-of-plane motion was measured to be approx. 30 nm for 4 µm of scan motion, without significant out-of-plane resonances in the frequency region of operation. This design could be used as component of a nanopositioning system for probe-based archival applications, for which a small form factor is not a requirement (Kartik *et al*., 2010a).

A novel sensing concept based on the magneto-resistance (MR) has been developed that shows great promise towards achieving high-bandwidth and high-resolution position sensing. The key idea here is to translate the motion of the scanner into a change in the magnetic field as seen by an MR sensor. The MR-based position sensor is depicted schematically in Fig. 5. It consists of two active and two shielded

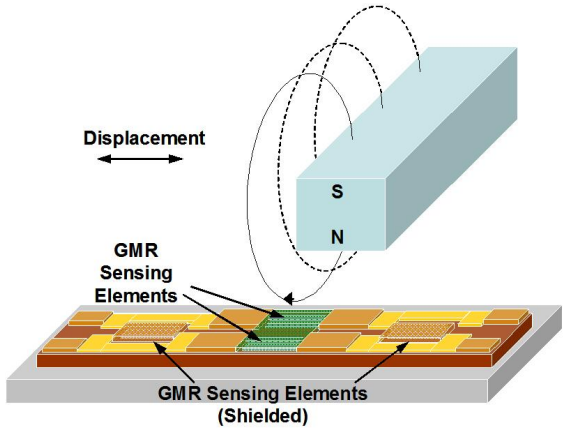

Fig. 5. Schematic depiction of magneto-resistance-based position-sensing concept. From Kartik *et al.* (2010a)

GMR sensing elements configured into a Wheatstone bridge. The sensor is sensitive in one direction in its plane, with a cosine scale-off in sensitivity as it is rotated away from its sensing direction. Two GMR sensors are mounted on the stationary frame of the scanner, one each for the *x*- and the *y*-axis. Two permanent magnets are glued to the moving scan table, again one for each axis, directly above the corresponding GMR sensors. As the scan table moves along each axis, the magnetic field seen by the corresponding GMR sensor changes. The resulting electrical resistance change is read using an analog low-noise circuitry. Because of the physical separation between the magnets and their orthogonal configuration, the coupling between the sensors for the *x*- and the *y*-axis is minimal. In the configuration depicted, a sensitivity of nearly 75 mV/m was achieved. The noise spectrum is largely dominated by 1/*f* noise, and the standard deviation of the noise integrated over the range 0–10 kHz is 0.177 mV, which corresponds to a spatial resolution of 2.36 nm. This is truly remarkable, given the simplicity of this sensing concept and the fact that this resolution is available over a bandwidth of 10 kHz (Kartik *et al*., 2010a).

2.2. Control strategies

Shaping of noise sensitivity transfer function. For data-storage applications, absolute positioning is needed, and hence one cannot rely only on a global position sensor that is susceptible to drift and low-frequency noise. Therefore, a medium-derived position-sensing concept was developed that provides positional information in the cross-track direction along the *y*-scan direction (Eleftheriou *et al.*, 2003; Pantazi *et al.*, 2007). The medium-derived positional information is obtained from a set of dedicated servo fields, on which specific servo patterns are inscribed prior to the regular operation of the device. This process is known as "self-servo-write" process, during which the scanner is moved in closed-loop mode, relying entirely on the thermal position sensors. However, during this self-servo-write process, subnanometer positioning accuracies are required, which are well below the resolution of these sensors. Therefore we exploited the concept of so-called directed shaping of the noise sensitivity transfer function to design feedback controllers that provide remarkably good positioning accuracies. The key idea was to control the scanner only in that frequency region in which control was essential. This made it possible to shape the noise sensitivity transfer function in such a way that the measurement noise does not impact the positioning accuracy in other frequencies (Sebastian *et al*., 2008b).

Two-sensor-based H_∞ control. During regular operation of the probe-storage device, positional information is available from the thermal position sensors and the servo fields. It is advantageous to use both of them together because the former can provide positional information over the entire scan range, whereas the medium-derived positional signal is not susceptible to drift and low-frequency noise. The trade-off in the noise performance of these two sensors was captured in an H_∞ control formulation to design a controller that relies on both sensors simultaneously to control the scanner. Using this control scheme, absolute positioning accuracies of less than a nanometer were achieved over a 100-µm range with a

disturbance rejection bandwidth of approx. 300 Hz (Pantazi *et al*., 2007). This nanopositioning work was a vital enabler in the demonstration of the highest areal density of 840 Gb/in^2 ever achieved in a probe-based data-storage device (Pantazi *et al*., 2008).

H_∞ control for high-bandwidth actuator. A closed-loop bandwidth of more than 1 kHz was achieved using the 2D piezo-actuated positioning stage and the magneto-resistance sensing presented in Section 2.1. The mechanical resonances were damped by means of a model-based H_∞ controller. The *x*- and the *y*-axis were controlled independently, and sixth-order models served to design the H_∞ controller for each axis. The requirements on the closed-loop transfer functions were specified in terms of first-order weighting functions. The experimental frequency responses of the closed-loop system for both the *x*- and the *y*-scan axis are shown in Fig. 6. Figure 7 shows the performance of the closed-loop system when a triangular scan operation at 250 Hz is performed along the *x*-scan direction while stepping in the *y*-scan direction by 100 nm. As both scan directions are controlled with very high bandwidths, the cross-coupling between the axes is minimal (Kartik *et al*., 2010a).

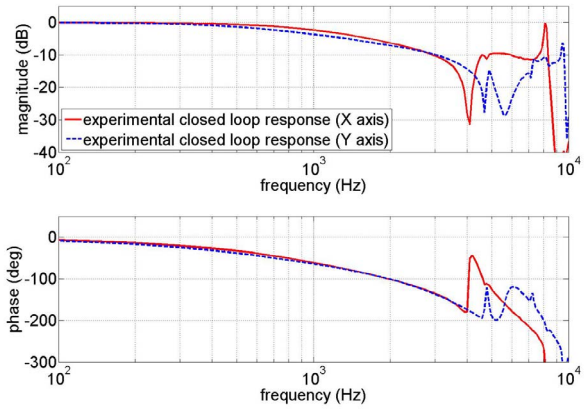

Fig. 6. Experimental closed-loop frequency response for *x*- and *y*-directions. From Kartik *et al.* (2010a)

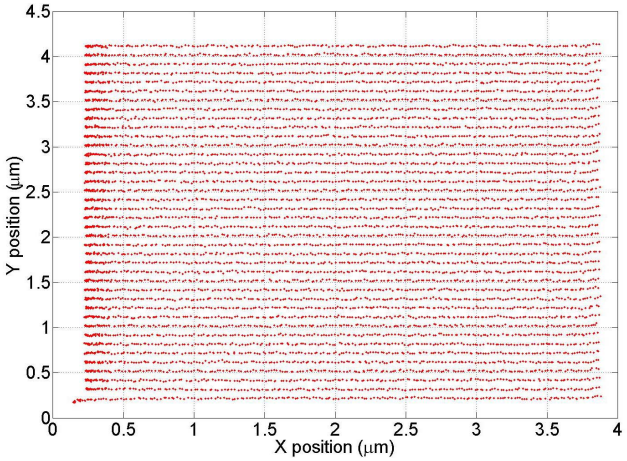

Fig. 7. Closed-loop scan operation along the *x*-direction while stepping in *y*-direction by 100 nm. From Kartik *et al.* (2010a)

Impulsive control for high-speed nanopositioning. Nonlinear control schemes can be used to overcome the inherent limitations of linear feedback control systems, such as the conflict between high-bandwidth tracking and low sensitivity to measurement noise. To that end, a novel nonlinear control scheme based on impulsive control was proposed that improves the tracking performance of a feedback loop without increasing the linear bandwidth of the controller. By doing so, the sensitivity to measurement noise is kept low and the positioning resolution is not compromised. In impulsive control, this is achieved by changing the controller states impulsively at discrete time instants, as shown in Fig. 8. Specifically, a particular type of impulsive control was introduced in which the state vector of a linear feedback controller is multiplied by a nonzero factor at specific time instances. This technique is well suited for tracking of piecewise affine reference signals, such as the triangular waveforms used in raster-based scanning. For this type of reference signals, the stability conditions and performance bounds of impulsive control were derived (Tuma *et al.*, 2011a) and prototype controllers were implemented which show great promise. For instance, in a high-speed AFM system, an impulsive controller significantly improved the tracking performance and led to better image quality, without increasing the bandwidth of the linear feedback loop (Tuma *et al.*, 2011b). Using the MEMS-based electromagnetic actuator presented in Section 2.1, fast raster tracking with a linear velocity of 1 mm/s and triangular reference signals of 100 Hz frequency was demonstrated. Figure 9 presents the performance in the steady state, showing that impulsive

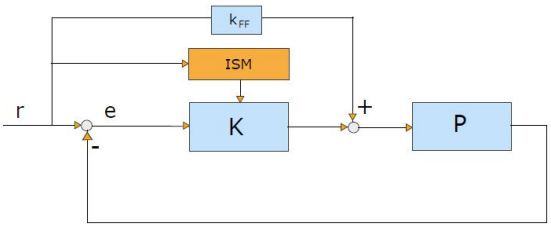

Fig. 8. Block diagram of impulsive control for nanopositioning. From Tuma *et al.* (2010)

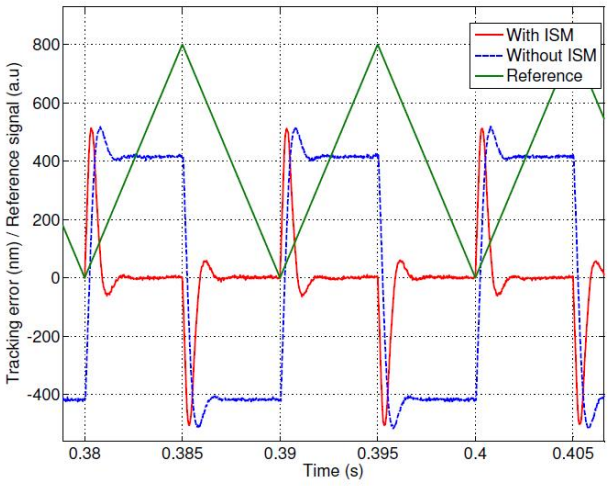

Fig. 9. Tracking error with and without impulsive control. Adapted from Tuma *et al.* (2010)

control enabled an improvement of the tracking by two orders of magnitude. Remarkably, the linear bandwidth of the feedback controller used in this experiment was less than 1 Hz (Tuma *et al.*, 2010).

3. TAPE STORAGE

The volume of digital data produced each year is growing at an ever-increasing pace. Moreover, new regulatory requirements imply that a larger fraction of this data will have to be preserved. All of this translates into a growing need for cost-effective digital archives. State-of-the-art commercial linear-tape products achieve an areal storage density of about 1 Gb/in^2 and a cartridge capacity on the order of one to two terabytes. Future scaling would require a dramatic increase in track density, which in turn implies nanoscale positioning of the head read/write transducers of a tape drive.

Tape recording is performed by writing magnetic transitions onto a thin, flexible medium that is being transported through a tape path. Rollers guide the tape from the cartridge reel over the head element to the take-up reel. The head is mounted on a positioning device, and the actuator and dedicated servo transducers on the head read the preformatted servo track information. Tape recording systems must be able to deal with effects originating from the moving flexible medium, guiding-system imperfections, and other tape-path characteristics that induce lateral tape motion (LTM). This LTM leads to a misalignment of the head read/write transducers with respect to the track locations. This is one of the key challenges tape control systems have to overcome to extend the capacity and performance limits of tape storage. The two main tape control systems, namely, the tape transport and the track-follow control system, are shown in the block diagram of Fig. 10. The tape transport system is responsible for maintaining a constant tape velocity and a constant tape tension while the tape is being transported from one reel to the other. The main task of the track-follow controller is to move the head such that it follows the LTM as accurately as possible during read/write operations. For this, the PES signal generated from the servo patterns recorded during manufacturing is used.

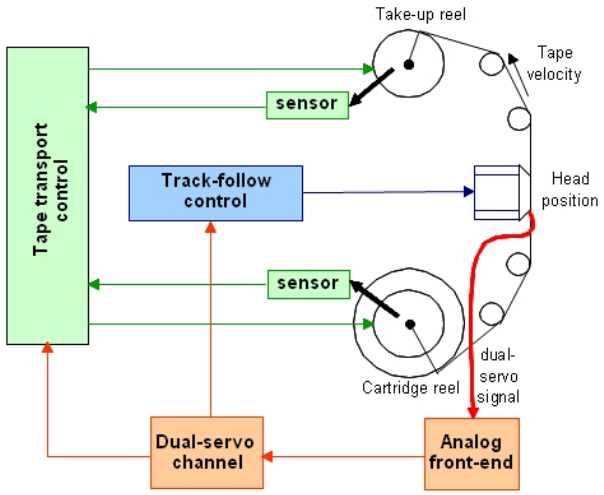

Fig. 10. Tape transport and track-follow control systems. From Pantazi *et al.* (2010)

3.1 Actuators and position sensing

Position-error signal. The position-error signal (PES) is employed to position the head actuator and is generated using the timing-based servo (TBS) method (Barrett *et al.*, 1998). TBS is a technology developed in the mid-1990s for linear tape drives and has been adopted in the Linear-Tape-Open (LTO) standard. The PES signal is generated based on the servo patterns recorded during manufacturing, which consist of transitions with two different azimuthal slopes, as shown in Fig. 11. The lateral position is derived from the relative timing of pulses generated by the head while reading the pattern. TBS patterns also serve to encode additional longitudinal position (LPOS) information by properly shifting transitions from their nominal pattern position using pulse-position modulation. Advanced servo-channel architecture schemes have been proposed to improve the resolution of the position and velocity estimates (Cherubini *et al.*, 2007).

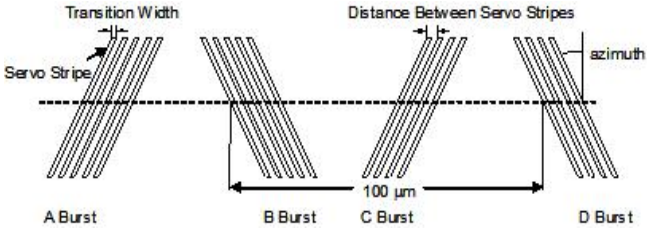

Fig. 11. Timing-based servo pattern. From Pantazi *et al.* (2010)

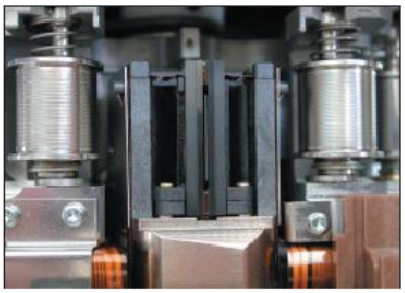

Fig. 12. Photograph of voice-coil head actuator assembly and rollers. Adapted from Biskeborn and Eaton (2003)

Voice-coil head actuator. The tape actuator is a two-stage actuator consisting of a high-bandwidth, low-mass, spring-mounted voice-coil and a heavier carrier driven by a stepper motor. A photograph of the head and actuator assembly is shown in Fig. 12. The moving mass of the voice-coil actuator is approx. 3 g, and it has displacement capabilities in the range of ±150 µm. The dynamics of the actuator are dominated by the fundamental resonance mode at approx. 78 Hz. There are some higher-order resonance modes above 10 kHz that are mostly due to the head cables. The task of the stepper motor is to bring the head within 15 µm of the target position, whereas the voice-coil-motor (VCM) actuator maintains track-following during read/write operations (Biskeborn and Eaton, 2003).

High-bandwidth piezoelectric actuator. To achieve a significant increase in track-follow performance, a high-bandwidth,

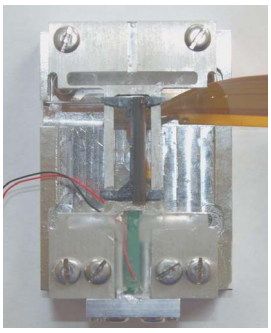

Fig. 13. Photo of piezoelectrically actuated track-following system. Adapted from Kartik *et al.* (2010b)

track-following actuator with piezoelectric actuation has been prototyped. This prototype, shown in Fig. 13, comprises a recording head mounted on a parallelizing flexure stage fabricated from aluminum. A piezoelectric stack is preloaded against the flexure and displaces it in response to an applied voltage. The stroke, stiffness, and blocking force of the piezo-stack are matched with the mass of the recording head and the stiffness of the flexure stage. A design compromise exists between the maximum achievable stroke and the capacitance and response time of the stack. The piezo-stack chosen generated a maximum (unloaded) stroke of 20 μm for an input voltage of 0–150 V and had a capacitance of 340 nF. The actuator was characterized by the frequency response in the direction of actuation obtained from the servo position estimation. The tape transport speed was 4 m/s. The response exhibits multiple peaks located in frequencies above 5 kHz (Kartik *et al*., 2010b).

3.2. Control strategies

Nanoscale track-following for flexible media. To investigate the achievable track-following performance with flexible tape media, advanced concepts for several elements of the tape system have been considered. One of the main factors limiting the tape track density is the lateral tape motion that is created when the tape is transported through the tape path from one reel to the other. The experimental setup consists of a commercial low-LTM tape transport system (Cherubini *et al*., 2011). The tape path consists of ten externally pressurized, porous ceramic air-bearing tape guides with hard-edge guiding. In combination with a long tape path, these guides, result in low LTM values with a standard deviation on the order of 1 μm. Advanced servo-control technologies have been considered for ultra accurate head positioning. First, a new servo-pattern geometry and a new method for detecting and decoding the position information minimized the measurement noise in the PES estimates. The track-follow controller was designed based on the H_∞ control framework, and the weights were selected according to the frequency characteristics of the LTM and the noise characteristics of the PES (Cherubini *et al*., 2011).

A block diagram of the experimental setup is shown in Fig. 14. The above technologies combined with new high-SNR magnetic tape with perpendicularly-oriented barium-ferrite magnetic medium enabled the demonstration of an extremely

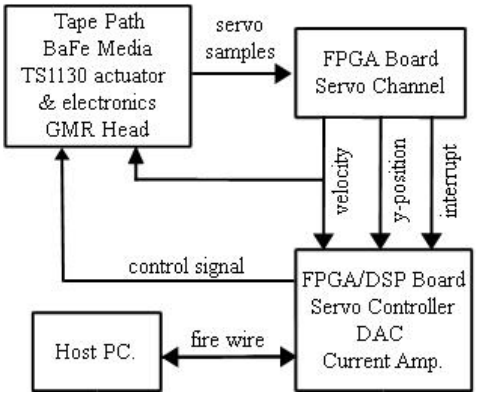

Fig. 14. Block diagram of experimental setup for track-follow experiments. From Cherubini *et al.* (2011)

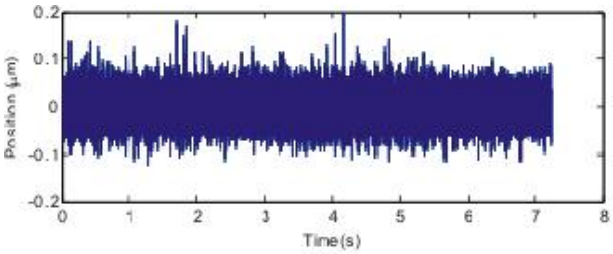

Fig. 15. Experimental results of closed-loop PES. From Cherubini *et al.* (2011)

precise track-follow performance of 23.4 nm standard deviation measured by the PES (Cherubini *et al*., 2011). Figure 15 presents the experimental capture of the closed-loop PES. In this experimental demonstration, the VCM actuator was used as track-follow head actuator. Simulation results of the high-bandwidth track-follow actuator with experimental waveforms, which were captured using the same tape path and the improved medium and servo pattern, showed that improvements in the positioning error on the order of 20 nm or less standard deviation are possible (Kartik *et al*., 2010b).

Track-follow control for LTM periodic components. In tape paths where the tape is transported through conventional flanged rollers, the LTM contains stationary periodic components. This is mostly due to run-outs, roller geometry imperfections, and other roller defects. The frequencies of the periodic disturbances appear at the rolling frequency and its harmonics, and depend on the tape-transport speed. Control architectures have been designed that exploit the knowledge of the disturbance frequencies to enhance the capabilities of the track-follow control system at these frequencies. An extended state-space model of the system has been developed that includes the actuator model and the disturbance characteristics, and a linear quadratic Gaussian (LQG) controller has been implemented based it. Figure 16 shows a comparison of the closed-loop transfer function for the LQG controller with improved disturbance rejection capabilities and a standard controller implementation. The experimental results in Fig. 17 demonstrate the improved performance in the closed-loop PES (Pantazi *et al*., 2010)

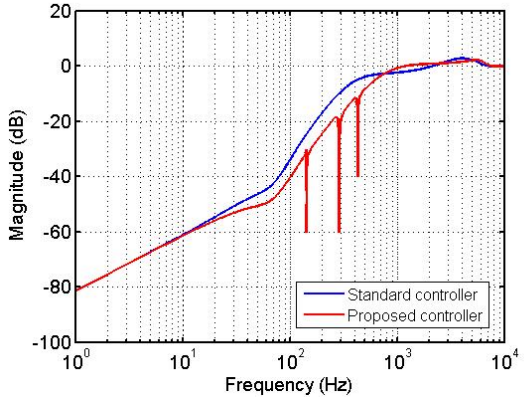

Fig. 16. Magnitude response of the closed-loop transfer functions. From Pantazi *et al.* (2010)

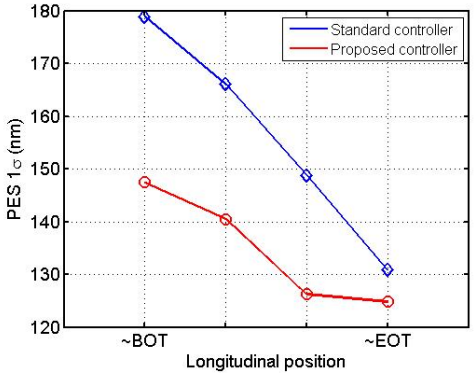

Fig. 17. Experimental results at different longitudinal positions ranging approximately from the beginning of tape (BOT) to the end of tape (EOT). From Pantazi *et al.* (2010)

Track-follow control for flangeless tape paths. The contact between roller flange and tape edge introduces high-frequency dynamic effects on the LTM. Such effects can be reduced by using a tape path with flangeless rollers, at the price of an increase of the low-frequency LTM. Specifically, effects called stack shifts are becoming more pronounced. During normal operation, a lateral displacement of a portion of the tape inside the tape pack can create a stack shift that appears as a low-frequency lateral displacement with high amplitude. To overcome this, a feed-forward enhancement to the track-follow control scheme is presented that uses information on the LTM captured by an optical edge sensor. This control architecture exploits the fact that in tape systems, disturbances originating at a specific location on the tape path will propagate through the path from one point to the other. This advance information on the LTM provided by the optical edge sensor can be used in the combined feed-forward and feedback control scheme illustrated in Fig. 18. Simulation results of the closed-loop system with and without feed-forward control are shown in Fig. 19. The scheme offers an improvement of approx. 40 nm in terms of the 1σ PES Specifically, with the feed-forward scheme, the 1σ PES could be reduced from 165 nm to 128 nm (Pantazi *et al*., 2010).

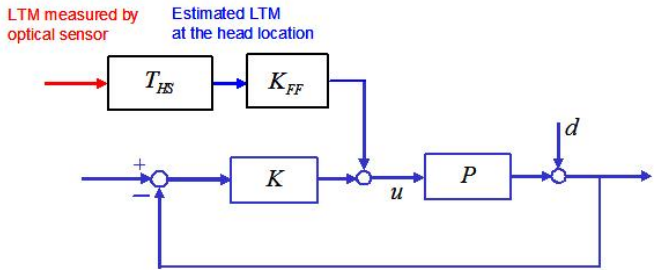

Fig. 18. Feed-forward control architecture. From Pantazi *et al.* (2010)

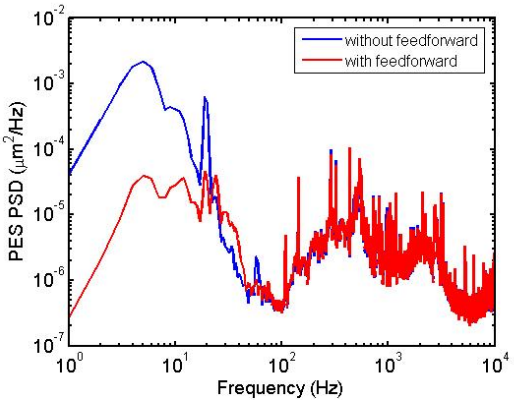

Fig. 19. Power spectral density of closed-loop PES with and without feed-forward control. From Pantazi *et al.* (2010)

4. CONCLUSIONS

The emerging field of nanotechnology has opened up new and challenging applications of control, specifically in nanopositioning. This paper reviewed the current status of actuators, position sensors, and control strategies that enable nanometer-scale precision control at dimensions below 100 nm for two extreme applications in data storage, namely, probe and tape storage. We showed that nanopositioning is crucial for achieving high areal densities and thereby large storage capacities in both applications.

ACKNOWLEDGMENTS

The author thanks his colleagues P. Bächtold, G. Cherubini, M. Despont, U. Drechsler, U. Egger, W. Häberle, J. Jelitto, V. Kartik, M. Lantz, A. Pantazi, H. Pozidis, H. Rothuizen, D. R. Sahoo, A. Sebastian and T. Tuma, for their contributions to the various aspects of scanning-probe and tape-drive technologies. Special thanks go to Angeliki Pantazi for her numerous comments and suggestions on this manuscript.

REFERENCES

Argumedo, A.J., *et al*. (2008). Scaling tape-recording areal densities to 100 Gb/in^2. *IBM J. Res. Develop.* **52**(4/5), 513-527.

Barrett, R.C., *et al.* (1998). Timing-based track-following servo for linear tape systems. *IEEE Trans. Magn.* **34**(4), part 1, 1872-1877.

Berman, D., *et al.* (2007). 6.7 Gb/in^2 recording areal density on barium ferrite tape. *IEEE Trans. Magn*. **43**(8), 3502-3508.

Bhaskaran, H., *et al.* (2009). Recent advances in conduction mode scanning probes for phase change probe storage applications. *Proc. European Symp. on Phase Change and Ovonic Science* (*E\PCOS 2009*) Aachen, Germany, `http://www.epcos.org/library/papers/pdf_2009/Bhaskaran%20et%20al%20Recent%20Advances.pdf`

Biskeborn, R.G., and J.H. Eaton (2003). Hard-disk-drive technology flat heads for linear tape recording. *IBM J. Res. Develop.* **47**(4), 385-400.

Bushan, B., Ed. (1995). *Handbook of Micro/Nano Tribology*. CRC, Boca Raton, FL.

Bushan, B., Ed. (2004). *Springer Handbook of Nanotechnology*. Springer-Verlag, Berlin, Germany.

Cherubini, G., *et al.* (2007). Synchronous servo channel design for tape drive systems. *Proc. 17th Ann. ASME Information Storage and Processing Systems Conf.,* Santa Clara, CA, pp. 160-162.

Cherubini, G., *et al*. (2011). 29.5 Gb/in^2 recording areal density on barium ferrite tape. *IEEE Trans. Magn*. **47**(1), 137-147.

Crandall, B.C. (1996). *Nanotechnology: Molecular Speculation on Global Abundance*. MIT Press, Cambridge, MA.

Croft, D., and S. Devasia (1999). Vibration compensation for high speed scanning tunneling microscopy. *Rev. Sci. Instrum*. **70**(12), 4600-4605.

Croft, D., G. Shed, and S. Devasia (2001). Creep, hysteresis, and vibration compensation for piezoactuators: Atomic force microscopy application. *ASME J. Dyn. Syst. Control* **123**(1), 35-43.

Devasia, S., E. Eleftheriou, and S.O.R. Moheimani (2007). A Survey of control issues in nanopositioning. *IEEE Trans. Control Syst. Technol.* **15**(5), 802-823.

El Rifai, O.M., and K. Youcef-Tomi (2001). Design and control of atomic force microscopes. *Proc. Amer. Control Conf. 2001*, pp. 3251-3255.

Eleftheriou, E., *et al*. (2003). "Millipede"—A MEMS based scanning-probe data storage system. *IEEE Trans. Magn*. **39**(2), 938-945.

Fleming, A.J., and S.O.R. Moheimani (2003). Precision current and charge amplifiers for driving highly capacitive piezoelectric loads. *Electron. Lett*. **39**(3), 282-284.

Harriot, L.R. (2001). Limits of lithography. *Proc. IEEE* **89**(3), 366-374.

Horowitz, R., *et al.* (2004). Microactuators for dual-stage servo systems in magnetic disk files. *Springer Handbook of Nanotechnology* (B. Bhushan, Ed.), ch. 31, pp. 921-950. Springer-Verlag, Berlin, Germany.

Hosaka, S., *et al.* (1997). SPM-based data storage for ultra-high density recording. *Nanotechnol.* **8**(3A), A58-A62.

Jianxu, M., and M.H. Ang, Jr. (2000). High-bandwidth macro /microactuation for hard disk drive. *Microrobotics and Microassembly II*, *Proc. SPIE,* vol. 4194, pp. 94-102.

Kalinin, S.V., and D.A. Bonnell (2000). Effect of phase transition on the surface potential of the $BaTiO_3$ (100) surface by variable temperature scanning surface potential microscopy. *J. Appl. Phys.* **87**(8), 3950-3957.

Kartik, V., *et al.* (2010a). High speed nanopositioner with magneto resistance-based position sensing. *Proc. 5th IFAC Symp. on Mechatronic Systems*, pp. 306-310.

Kartik, V., A. Pantazi, and M. Lantz. (2010b). High bandwidth track following for moving media. *Proc. 20th ASME Information Storage and Processing Systems Conf*., pp. 265-267.

Krogmann, D., *et al*. (1999). Image multiplexing system on the base of piezoelectrically driven silicon microlens arrays. *Proc. 3rd Int. Conf. Micro Opto Electro Mechan. Syst. (MOEMS)*, pp. 178-185.

Lantz, M.A., G.K. Binnig, M. Despont, and U. Drechsler (2005). A micromechanical thermal displacement sensor with nanometer resolution. *Nanotechnol.* **16**, 1089-1094.

Lantz, M.A., *et al.* (2007). A vibration resistant nanopositioner for mobile parallel-probe storage applications. *J. Microelectromech. Syst.* **16**, 130-139.

Meldrum, D.R., *et al*. (2001). Automated, integrated modules for fluid handling, thermal cycling and purification of DNA samples for high throughput sequencing and analysis. *Proc. IEEE/ASME Int. Conf. Adv. Intell. Mechatron*., pp. 1211-1219.

Pantazi, A., *et al.* (2007) Control of MEMS-based scanning-probe data-storage devices. *IEEE Trans. Control Syst. Technol.* **15**, 824-841.

Pantazi, A., *et al.* (2008). Probe-based ultrahigh-density storage technology. *IBM J. Res. Develop.* **52**(4/5), 493-511.

Pantazi, A., J. Jelitto, N. Bui, E. Eleftheriou (2010).Track-follow control for tape storage. *Proc. 5th IFAC Symposium on Mechatronics Systems,* pp. 532-537.

Rihong, Z., X. Daocai, Y. Zhixing, and C. Jinbang (1998). Research on systems for measurements of CCD parameters. *Detectors, Focal Plane Arrays, Imaging Devices II*, *Proc. SPIE*, vol. 3553, pp. 297-301.

Salapaka, S., A. Sebastian, J.P. Cleveland,. and M.V. Salapaka (2002). High bandwidth nano-positioner: A robust control approach. *Rev. Sci. Instrum*. **73**(9), 3232-3241.

Sebastian, A., and S.M. Salapaka (2005). Design methodologies for robust nano-positioning. *IEEE Trans. Control Syst. Technol.* **13**(6), 868-876.

Sebastian, A., A. Pantazi, H. Pozidis, and E. Eleftheriou, (2008a). Nanopositioning for probe-based data storage. *IEEE Control Syst. Mag.* **28**(4), 26-35.

Sebastian, A., *et al.* (2008b). Achieving subnanometer precision in a MEMS-based storage device during self-servo write process. *IEEE Trans. Nanotechnol.* **7**(5), 586-595.

Schitter, G., *et al.* (2001). High performance feedback for fast scanning atomic force microscopes. *Rev. Sci. Instrum*. **72**(8), 3320-3327.

Shapiro, B. (2005). Workshop on control of micro- and nano-scale systems. *IEEE Control Syst. Mag*. **25**(2), 82-88.

Sheetz, T., J. Vidal, T.D. Pearson, and K. Lozano (2005). Nanotechnology: Awareness and societal concerns. *Technol. Soc.* **27**(3), 329-345.

Stemmer, A., G. Schitter, J.M. Rieber, and F. Allgoewer (2005). Control strategies towards faster quantitative imaging in atomic microscopy. *Eur. J. Control* **11**, 384-395.

Tuma, T., A. Pantazi, J. Lygeros, and A. Sebastian. (2010). Tracking of high frequency piecewise affine signals using impulsive control. *Proc. 5th IFAC Symp. on Mechatronic System*s, pp. 90-95.

Tuma, T., A. Pantazi, J. Lygeros, and A. Sebastian (2011a). Impulsive control for nanopositioning: stability and performance. *Proc. 14th Int'l Conf. on Hybrid Systems: Computation and Control (HSCC'11),* in press.

Tuma, T., *et al.* (2011b). Impulsive control for fast nanopositioning. *Nanotechnol*. **22**, 135501.

Verma, S., W.-J. Kim, and H. Shakir (2005). Multi-axis maglev nanopositioner for precision manufacturing and manipulation applications. *IEEE Trans. Ind. Appl.* **41**(5), 1159-1167.

Vettiger, P., *et al.* (2002). The "millipede"—nanotechnology entering data storage. *IEEE Trans. Nanotechnol*. **1**, 39-55.

Vettiger, P., U. Staufer, and D.P. Kern, Eds. (1996). *Microelectron. Eng.* **32**(1-4), special issue on Nanotechnology.

White, D.L., and O.R. Wood (2000). Novel alignment system for imprint lithography. *J. Vac. Sci. Technol. B* **18**(6), 3552-3556.

Whitesides, G.M., and H.C. Love (2001). The art of building small. *Scientific Amer.* **285**(3), 39-47.

Wiesendanger, R., Ed. (1994). *Scanning Probe Microscopy and Spectroscopy*. Cambridge Univ. Press. Cambridge, UK.

Wright, C.D., M. Armand, and M.M. Aziz (2006). Terabit-per-square-inch data storage using phase-change media and scanning electrical nanoprobes. *IEEE Trans. Nanotech*. **5**(1), 50-61.

Wright, C.D., *et al*. (2008). Scanning probe-based phase-change terabyte memories. *European Phase Change and Ovonics Symposium* (*E\PCOS 2008*), Prague, Czech Republic, http://www.epcos.org/library/papers/pdf_2008/Oral/Wright.PDF

Yves, M. (1995). *Scanning Probe Microscopes*. SPIE, Bellingham, WA.